Water Resour Manage (2011) 25:2797–2822
DOI 10.1007/s11269-011-9839-5

Application of the Regional Flood Frequency Analysis to the Upper and Lower Basins of the Indus River, Pakistan

Zamir Hussain

Received: 24 October 2009 / Accepted: 2 May 2011 /
Published online: 24 May 2011

Abstract The paper presents results of an application of the L-moments based regional flood frequency analysis to annual maximum peak (AMP) flows observed at seven stations (Tarbela, Kalabagh, Chashma, Taunsa, Guddu, Sukkur and Kotri) located on the main stream of the Indus River, Pakistan. The results of Run-test and lag-1 correlation coefficient showed that the data series at given sites is random and has no serious serial correlations respectively. Furthermore, the results of Grubbs and Beck test illustrated that there are no irregularities (abrupt variations) except low outlier(s) in the data series at various sites. To avoid their undue influence, these low outliers have been discarded and the sample information has been re-summarized using the idea of left censored type A' partial probability weighted moments. L-moments based regional heterogeneity measure (H) showed that the region, defined by seven stations, is heterogeneous; therefore, it has been sub-divided into two homogeneous regions (Region 1 and Region 2 consist of four (Tarbela, Kalabagh, Chashma and Taunsa) and three sites (Guddu, Sukkur and Kotri, respectively) using Ward's clustering method based on the site characteristics only. The results of various goodness-of-fit measures (L-moment ratio diagram, average weighted distance and Z^{DIST} measures) showed that Region 1 has four candidates: generalized normal (GNO), generalized logistic (GLO), generalized extreme-value (GEV) and Pearson type III (PE3), while Region 2 has only one candidate; GLO, as regional distribution. Based on the results of different accuracy measures (regional average absolute relative bias, relative bias and relative root mean square error) of the estimated regional growth curves and quantiles, obtained from simulation experiments, PE3 is the robust distribution for Region 1, while for Region 2, GLO distribution can be used for the estimation of flood quantiles. Moreover, the results of the simulations study have been extended to obtain standard errors of the estimated quantiles at each site of the sub-divided homogeneous regions.

Z. Hussain (✉)
Department of Statistics, Bahauddin Zakariya University, Multan, Pakistan
e-mail: zami_cr@yahoo.com

Keywords Indus river · L-moments · Partial probability weighted moments · Regional frequency analysis · Ward's clustering method

1 Introduction

Pakistan has one of the largest integrated river basins in the world, with the Indus River as its backbone and considered to be the lifeline of Pakistan. Not only the river has its prime importance in the river basins of Pakistan but also has the recognition among the biggest rivers in the world. Its drainage basin area is of the order of 9.7×10^5 km^2, making it the 12th largest, deltaic area is 3×10^4 km^2, ranking it 7th, annual water runoff is a little under 2×10^{11} m^3/year, placing it 10th and annual sediment discharge is 2×10^{11} kg/year, placing it 6th, among the rivers of the world (Pakistan Water Gateway 2008). In addition, the country has an agro based economy and arid or semi-arid climatic conditions, therefore, accurate estimates of flood quantiles becomes an integral part of the design and operation of water resource systems, land use planning and management, flood insurance assessment and protection of inhabited areas, etc. Previously documented frequency analyses were performed either by fitting a probability distribution or applying regression approach to observed flow data at a single site with short records, for example Khattak (1994), Musa (1999), Hussain (2000), Govt. of Pakistan (2001), Jehanzeb (2004), Memon (2006, 2007), Muhammad and Afreen (2007), Shujah (2009), therefore, it is important to revise these estimates using additional data and new approaches. At-site frequency methods can suffer from sampling variability, especially for estimating return periods that exceed the length of the observed record at a site (Cunnane 1988; Hosking and Wallis 1993).

One way of providing more reliable estimates is to use several records from a region with identical behavior of flood statistics. This is known as regional flood frequency analysis. The regional approach not only provides accurate and reliable flood quantile estimates at gauged sites but also the results can be used for the estimation of flood quantiles at ungauged sites. Several authors investigated the regional frequency analysis procedure in various hydro-climatic settings, e.g. Stedinger and Tasker (1986), Burn (1990), Hosking and Wallis (1993), Durrans and Tomic (1996), Nguyen and Pandey (1996), Ouarda et al. (2001), for floods and Alila (1999, 2000), for precipitation extremes. An inter-comparison of various regional flood estimation procedures was presented by GREHYS (1996a, b).

L-moments based regional frequency analysis is practiced all over the world (for example, Guttman et al. 1993; Smithers and Schulze 2001; Ben-Zvi and Azmon 1997; Pandey et al. 2001; Elamir and Seheult 2001; Jingyi and Hall 2004; Saf 2009; Eslamian and Feizi 2007; Modarres 2007; Norbiato et al. 2007; Hussain and Pasha 2009; Castellarin et al. 2008; Yang et al. 2009) but an important aspect, in the comparison of quality of the quantile estimates obtained at each site from regional approach to that of at-site analysis, is how can we calculate the standard errors of the estimated quantiles at each site of a homogeneous region? In this paper, a relationship provided in Hosking and Wallis (1997) has been explored and standard errors of the estimated flood quantiles at each site of the homogeneous regions have been calculated by extending the results of the simulation experiments related to the accuracy measures

of the regional estimates. These standard errors will facilitate to compare the quality of the quantile estimates at each site resulting from L-moments based regional approach to that of other approaches for the frequency analysis of extreme events. Furthermore, Hussain and Pasha (2009) performed L-moments based regional flood frequency analysis of the seven sites of the eastern tributaries of the Indus River but the regional approach has never been adopted for the estimation of flood quantiles at various sites of the Indus River. Therefore, a detailed and comprehensive analysis is due.

The rest of the paper is organized as follows: Section 2 provides description of the area of study and available data for the analysis. Section 3 contains the theoretical background of L-moments, left censored partial probability weighted moments and various measures related to the procedure of regional frequency analysis. Section 4 deals with the results of the application of L-moments based regional flood frequency analysis to the sites of the Indus River, Pakistan. Section 5 is devoted to the comparison of results of the current study with the previously documented at-site analyses. Summarizing and concluding remarks are presented in Section 6.

2 Area of Study and Data Availability

Geographically, Pakistan is a mixture of landscapes varying from mostly plains to deserts, forests, hills and plateaus ranging from the coastal areas of the Arabian Sea in the south to the world's highest mountains in the north. The study area includes the sites of the most important, complex and biggest river of the river basins of Pakistan namely: the Indus. Stretching in the north, from east to west, are the series of high mountain ranges; namely Himalayas, Karakoram and Hindu Kush. These mountains with their unbroken snow cover become the primary source of water to the Indus system. This area, not only includes some of the world's highest peaks (for example, K2) but also have some of the longest glaciers (for example, Baltoro and Pasu). South of the northern highlands and west of the Indus River plain, are the barren mountain ranges namely: Safed Koh, Sulaiman and the Kirthar. The lower basin of the Indus River, especially after the join of the four major eastern tributaries (Jhelum, Chenab, Ravi and Sutlej), the area consists of arid plains of Punjab and Sindh.

AMP flows of the available seven sites of the Indus River have been used for the study. Data has been retrieved from the hydrology department of Water and Power Development Authority (WAPDA; which is responsible to record and update the flow information of various gauging sites of the river basins of the country) and National Engineering Services Pakistan (Pvt.) Limited (NESPAK). Summary statistics of the observed AMP flows have already been used by WAPDA and NESPAK in their technical reports. Geographical locations of the sites (as per their sequence number in Table 1) are illustrated in Fig. 1.

Site characteristics of the seven sites are illustrated in Table 1. The four available site characteristics are: average annual precipitation (AAP), average precipitation during monsoon (APDM), site's latitude and site's longitude. It has been observed that the sites have latitude between 25° to 34° North and longitude between 68° to 73° East. The variables, AAP and APDM, have been observed from 30-years

Table 1 Site characteristics of seven sites of the Indus River

No.	Site Name	AAP (mm)	APDM (mm)	Latitude (North)	Longitude (East)
1	Tarbela	1000	700	33.99	72.61
2	Kalabagh	300	225	32.95	71.50
3	Chashma	300	225	32.43	71.38
4	Taunsa	175	100	30.50	70.80
5	Guddu	125	75	28.30	69.50
6	Sukkur	125	75	27.72	68.79
7	Kotri	150	100	25.22	68.22

NORMALS (isohyetal) maps prepared by Pakistan Meteorological Department (PMD), Islamabad (Pakistan Meteorological Department 2010). These maps are based on the past 30 year's precipitation records (1961–1990) at different locations all over the country.

Fig. 1 Geographical locations of seven sites of the Indus River

3 Methodology

3.1 L-moments

The concept of L-moments originates from various previous studies on linear combinations of order statistics, e.g. Sillitto (1969), David (1968), Chernoff et al. (1967) and Greenwood et al. (1979). Hosking (1990) unified the theory of L-moments and provided guidelines for the practical use of L-moments. L-moments are special cases of probability weighted moments (PWM) but have an advantage to interpret directly as measures of scale and shape. As an alternative to conventional moments, L-moments, generally, have better statistical properties. Their asymptotic approximations to sampling distributions are better in comparison to the conventional moments. They are also robust to outlying values of data and provide better identification of the parent distribution that generated a particular sample of data (Hosking 1990).

PWM defined by Greenwood et al. (1979) are the quantities

$$M_{p,r,s} = \mathrm{E}\left[x^p \{F(x)\}^r \{1 - F(x)\}^s\right] \tag{1}$$

Where p, r and s are real numbers and $F(x)$ is the cumulative distribution function of x. A useful case is $\beta_r = M_{1,r,0}$. For a distribution that has a quantile function $x(F)$

$$\beta_r = \int_0^1 x(F)\, F^r dF \tag{2}$$

L-moments are linear combinations of PWM. The rth L-moment λ_r is related to the rth PWM through:

$$\lambda_{r+1} = \sum_{k=0}^{r} \beta_k (-1)^{r-k} \binom{r}{k} \binom{r+k}{k} \tag{3}$$

Hosking (1990) defined L-moment ratios as:

$$\mathrm{L-CV}: (\tau) = \lambda_2/\lambda_1\,, \tag{4}$$

$$\mathrm{L-skewness}: (\tau_3) = \lambda_3/\lambda_2, \tag{5}$$

$$\mathrm{L-kurtosis}: (\tau_4) = \lambda_4/\lambda_2. \tag{6}$$

The corresponding sample L-moments are denoted by l_r and sample L-moment ratios by t, t_3 and t_4.

3.2 Partial Probability Weighted Moments for Left Censoring

While working with the data sets related to flood, drought or precipitation events, it is not uncommon to obtain data points that are below some threshold value. In the frequency analysis of extreme events such data points are of little interest and can be a nuisance to the fitting process, therefore, sometimes it is advantageous to intentionally censor (or discard) such observations in order to better understand

the frequency and magnitude of floods and droughts (Wang 1990a, b, 1996; Durrans 1996).

The concept of partial probability weighted moments (PPWMs) was first introduced by Wang (1990a, b, 1996). The aim was to get rid of smaller observations for fitting a distribution. Zafirakou-Koulouris et al. (1998) derived PPWMs for type A' left censoring, using the same approach of Hosking (1995) for right censoring. The type A' PPWM of a left-censored distribution is the ordinary PWM of a (complete) distribution with quantile function

$$y^{A'}(F) = x(\phi),\ 0 < F < 1. \tag{7}$$

and is given by

$$\beta_r^{A'} = \frac{1}{(1-c)^{r+1}} \int_c^1 x(F)(F-c)^r\, dF, \tag{8}$$

where "c" is the fraction of observations which are censored. An unbiased estimator of type A' PPWMs for left censored observations is

$$b_r^{A'} = \frac{1}{k} \sum_{j=1}^{k} \frac{(j-1)(j-2)\ldots(j-r)}{(k-1)(k-2)\ldots(k-r)} X_{n-k+j:n},\ k = n-m+1. \tag{9}$$

Unbiased type A' L-moments for left censoring are obtained by substitution of $b_r^{A'}$ in place of b_r in Eq. 3.

3.3 The Discordancy Measure

Hosking and Wallis (1997) proposed a discordancy measure (D_i) based on L-moments, to recognize those sites that are grossly discordant with the group as a whole.

For a group containing N sites, the D_i for site i is defined as

$$D_i = \frac{1}{3} N (u_i - \overline{u})^T S^{-1} (u_i - \overline{u}),\ i = 1, 2, \ldots, N, \tag{10}$$

where $u_i = \left[\mathrm{t}^{(i)}\ \mathrm{t}_3^{(i)}\ \mathrm{t}_4^{(i)} \right]^{\mathrm{T}}$,

S matrix of sums of squares and cross products,
$\overline{u}$ mean of vector u_i.

Site i is said to be discordant if D_i value is large. Critical values for D_i are available in table form in Hosking and Wallis (1997).

3.4 Regional Heterogeneity Measure

To estimate the degree of heterogeneity in a group of sites, Hosking and Wallis (1997) proposed a heterogeneity measure (H). For a region containing N sites, with site i having record length n_i and sample L-moment ratios $t^{(i)}, t_3^{(i)}$ and $t_4^{(i)}$. The between-site variation of L-moment ratio is measured as the standard deviation (V) of the at-site sample L-CVs weighted proportionally to the site's record length. To

establish "what would be expected on average", we rely on simulations. Based on the regional weighted measures, a number of, say 500 data regions are generated with sites having record lengths the same as those of the observed data. These simulations are undertaken using a four-parameter Kappa distribution (Hosking and Wallis 1997). H can be computed from

$$H = \frac{V - \mu_V}{\sigma_V}, \tag{11}$$

where μ_V and σ_V are the mean and the standard deviation of the values of V obtained from simulations. A region is acceptably homogeneous if $H < 1$, possibly heterogeneous if $1 \leq H < 2$ and definitely heterogeneous if $H \geq 2$.

3.5 Choice of a Regional Frequency Distribution

3.5.1 L-moment Ratio Diagram

It is a plot of L-skewness (τ_3) versus L-kurtosis (τ_4), which is a useful guideline for the selection of an appropriate distribution for describing a set of variables as a distinct relationship between L-moment ratios exists for each theoretical probability distribution. These diagrams are more useful in identifying the candidate distributions to describe regional data in comparison to the ordinary product moment diagrams (Vogel and Fennessey 1993). However, choice of a best fitted distribution using L-moment ratio diagram depends on homogeneity of the regional data (Peel et al. 2001).

3.5.2 Average Weighted Distance Measure

By comparing sample L-moment ratios to the population ones via the L-moment ratio diagram, one may be able to obtain the best fit distribution for representing sample data. But this visual assessment is somewhat subjective and it is not possible to distinguish the differences when two or more distributions seem to be possible candidates in an L-moment ratio diagram (Peel et al. 2001). To overcome this problem, the average weighted distance (AWD) method of Kroll and Vogel (2002) has been used to measure the differences between sample and theoretical L-moment ratios. The AWD measure is defined as:

$$AWD = \frac{\sum_{i=1}^{N} n_i d_i}{\sum_{i=1}^{N} n_i}, \tag{12}$$

where $d_i = \left|\tau_4\left[t_3^0(i)\right] - t_4^0(i)\right|$, N is number of sites in the analysis, n_i is record length at each site, $t_4^0(i)$ is sample L-kurtosis at each site and $\tau_4\left[t_3^0(i)\right]$ is the theoretical L-kurtosis values calculated from a distribution corresponding to a given sample L-skewness. A distribution having smallest AWD value is considered to be the best candidate distribution for to the sample data.

3.5.3 Z^{DIST} Statistic Criteria

Hosking and Wallis (1997) proposed an expedient method for the goodness of fit of a given distribution. The measure of goodness of fit for a distribution is defined by

$$Z^{DIST} = \left(\tau_4^{DIST} - t_4^R + B_4\right)/\sigma_4, \tag{13}$$

where τ_4^{DIST} is L-kurtosis of the fitted distribution, t_4^R is weighted regional average L-kurtosis, B_4 is the bias of t_4^R and σ_4 is the standard deviation of the t_4^R obtained from simulations. For a given distribution, a satisfactory fit is the one with $\left|Z^{DIST}\right| \leq 1.64$. It may happen that a number of distributions can qualify this goodness of fit criteria. Then the most suitable distribution will be the one with minimum $|Z^{DIST}|$ value.

3.6 Estimation of the Regional Frequency Distribution

After the selection of suitable regional frequency distribution(s), the next obvious step is the estimation of parameters and quantiles of the respective distribution(s). A procedure stated in Hosking and Wallis (1997), based on the index-flood method, has been adopted. The estimates of quantiles, with nonexceedance probability F, for each site can be obtained by:

$$\hat{Q}_i(F) = l_1^{(i)} \hat{q}(F). \tag{14}$$

Where $\hat{q}(F)$ is the quantile function (standardized quantile function) of the fitted regional frequency distribution.

3.7 Assessment of Accuracy of the Estimated Regional Quantiles and Growth Curves

In order to quantify the accuracy of the estimates obtained by regional frequency analysis, we need certain measures of accuracy of these estimates. An algorithm based on the Monte Carlo simulations for the assessment of accuracy of the estimated regional quantiles and growth curves has been provided by Hosking and Wallis (1997; "Section 6.4").

In the simulation procedure, quantile estimates are calculated for various nonexceedance probabilities. At the *mth* repetition, site-*i* quantile estimate for nonexceedance probability F is $\hat{Q}_i^{[m]}(F)$. The relative error of this estimate at site i for nonexceedance probability F is $\left\{\hat{Q}_i^{[m]}(F) - \hat{Q}_i(F)\right\}/\hat{Q}_i(F)$. To approximate the bias and relative root mean square error of the estimators, these quantiles can be averaged over all M repetitions. So, the relative bias and relative root mean square error can be specified as percentages of the site i quantile estimator by

$$B_i(F) = M^{-1} \sum_{m=1}^{M} \frac{\hat{Q}_i^{[m]}(F) - \hat{Q}_i(F)}{\hat{Q}_i(F)} \tag{15}$$

and

$$R_i(F) = \left[M^{-1} \sum_{m=1}^{M} \left\{ \frac{\hat{Q}_i^{[m]}(F) - \hat{Q}_i(F)}{\hat{Q}_i(F)} \right\}^2 \right]^{1/2}. \tag{16}$$

The regional average absolute relative bias, relative bias and relative root mean square error of the estimated quantile are

$$A^R(F) = N^{-1}\sum_{i=1}^{N}|B_i(F)|, \tag{17}$$

$$B^R(F) = N^{-1}\sum_{i=1}^{N}B_i(F), \tag{18}$$

and

$$R^R(F) = N^{-1}\sum_{i=1}^{N}R_i(F). \tag{19}$$

Analogous quantities can be calculated for the estimates of growth curve, but with $\hat{Q}_i(F)$ and $\hat{Q}_i^{[m]}(F)$ replaced by $\hat{q}_i(F)$ and $\hat{q}_i^{[m]}(F)$ respectively. 90% error bounds for $\hat{q}(F)$ are

$$\frac{\hat{q}(F)}{U_{0.05}(F)} \le q(F) \le \frac{\hat{q}(F)}{L_{0.05}(F)} \tag{20}$$

Where $L_{0.05}(F)$ and $U_{0.05}(F)$ are the values between which approximately 90% of the distribution of simulated values of ratio of estimated to true values of regional quantile function, i.e. $\hat{q}_i(F)/q_i(F)$, lies. Details can be seen in Hosking and Wallis (1997).

4 Results of the Study

4.1 Time Series Plots and Test of Randomness

In order to investigate the pattern of variability in a data series, a visual inspection is always handy. Time series plots provide an initial clue about the likely nature of the series. These plots, of AMP flows at each site of the Indus River, are presented in Fig. 2. In general, the data series at all the sites showed no regular jumps or trends. After the visual inspection, it can be concluded that there is no uniform increasing/decreasing trend in the data series of seven sites of the Indus River.

To check for randomness of the data series at given sites, a non-parametric test, i.e. Run-test (Bradley 1968), has been applied and the results are presented in Table 2. For each site, the corresponding p-value of *ONR* (the observed number of runs) suggested that the hypothesis of randomness of the data series cannot be rejected at 5% level of significance.

4.2 Lag-1 Correlation Coefficient

To check for the existence of serial correlation in the data series at given sites, lag-1 correlation coefficient (r_1) (Kendal and Stuart 1968) has been used and the values of r_1, for each site, are given in Table 2. All these values indicate that there is no evidence of serious serial correlation in the data series at any site. The highest value is 0.2121, at site "Chashma". Hosking and Wallis (1997) concluded that a small

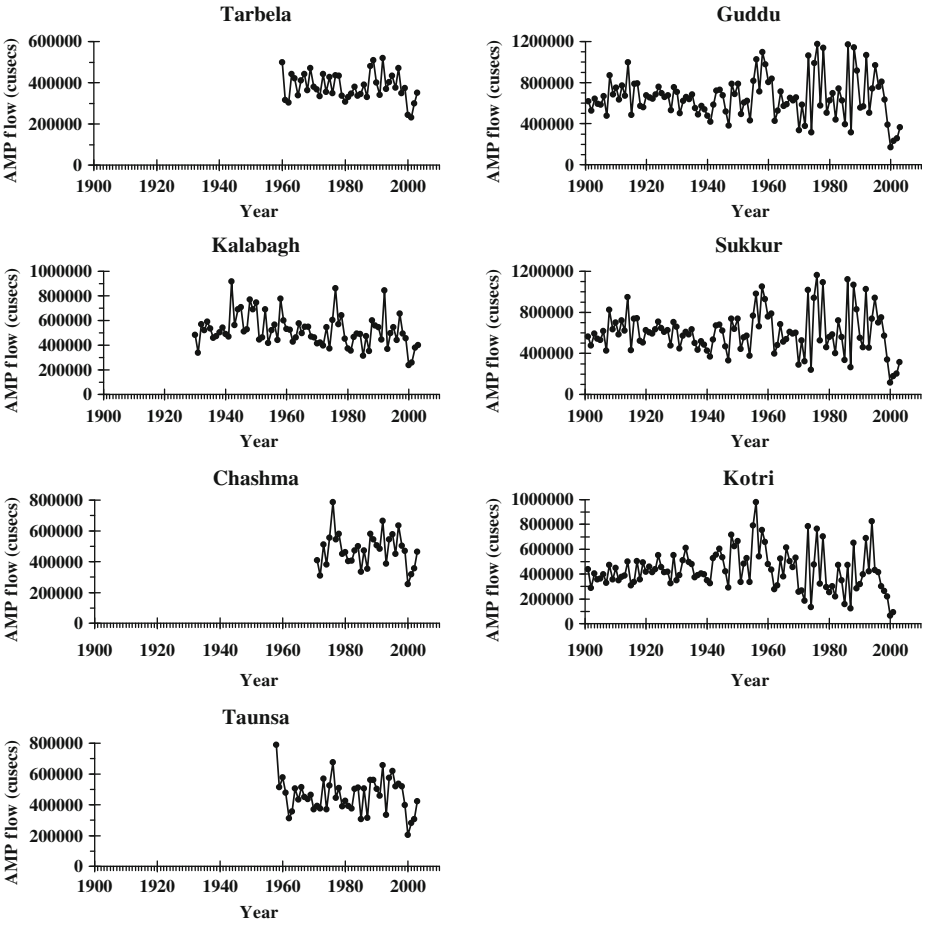

Fig. 2 Time series plots of seven sites of the Indus River

Table 2 Values of the lag-1 correlation coefficient, G–B and Run tests at each site of the Indus River

Site Name	n	r_1	k_n	x_H (cusecs)	x_L (cusecs)	NHO	NLO	ONR	P value
Tarbela	44	0.1570	2.7191	608565	231761	0	1	24	0.5855
Kalabagh	74	0.1988	2.9122	1044760	241977	0	1	31	0.1113
Chashma	33	0.2121	2.6038	862119	247041	0	0	13	0.1195
Taunsa	46	0.1700	2.7363	903000	221299	0	1	24	1.0000
Guddu	103	0.0449	3.0272	1748216	219910	0	1	45	0.1485
Sukkur	103	0.0422	3.0272	1830316	174395	0	1	45	0.1485
Kotri	101	0.1591	3.0206	1493414	106655	0	2	48	0.5570

x_H and x_L are the upper and lower thresholds for the detection of outliers, NHO and NLO are number of high and low outliers in the data series, respectively. P value is the corresponding probability for the acceptance/rejection of null hypothesis of randomness

amount of serial dependence in annual data series has little effect on the quality of the estimates. Therefore, the statement that the data series at seven sites have no serious serial correlation seems appropriate.

4.3 Detection of Outliers

The Grubbs and Beck (1972) test (G–B) has been used for the detection of outliers in the data series. In order to calculate k_n (the G–B statistic), an approximation stated in Rao and Hamed (2000), at 10% level of significance, has been used, i.e.

$$k_n = -3.62201 + 6.28446n^{1/4} - 2.49835n^{1/2} + 0.491436n^{3/4} - 0.037911n. \quad (21)$$

Where n is the sample size. For each site, the results are illustrated in Table 2, which shows that the data series do not have high outliers at any site. Low outlier(s) has been observed in the data series at various sites except Chashma.

4.4 The discordancy measure

In order to check for any discordant site in the group of seven sites, the discordancy measure (D_i), described in Eq. 10, has been calculated and the D_i values alongwith the sample L-moment ratios, for each site, are illustrated in Table 3. None of the site has D_i value greater than the critical value suggested by Hosking and Wallis (1997), i.e. 1.92, therefore, it can be concluded that there is no discordant site in the region.

In Table 3, the pattern of the values of l_1 (mean of AMP flows at each site) is interesting. The three major factors contributing in the high variations between these values are, (1) the length of the Indus River (the total length of the Indus River is 3,180 km out of which approximately 2,066 km flows in Pakistan, (2) the contribution of the eastern and western tributaries at various locations of the Indus River, and (3) the variation in the record length at each site.

4.5 Formation of Homogeneous Regions

After the preliminary screening of the data series at given sites, the next important step in regional flood frequency analysis is the formation of homogeneous region(s), that is, grouping sites with similar second and higher-order statistics, apart from a site specific scale factor. This step has prime importance and a fundamental requirement

Table 3 Summary statistics of annual maximum peak flows of seven sites of the Indus River

Site Name	n	l_1	t	t_3	t_4	D_i
Tarbela	44	381250	0.0980	0.0631	0.1237	1.64
Kalabagh	74	518521	0.1374	0.1402	0.2166	1.67
Chashma	33	474263	0.1323	0.0471	0.1691	0.79
Taunsa	46	461086	0.1382	0.0285	0.1418	0.74
Guddu	103	654190	0.1746	0.0873	0.2001	0.31
Sukkur	103	603920	0.1912	0.0887	0.1989	0.40
Kotri	101	432988	0.2083	0.1050	0.1867	1.45

n record length, l_1 first sample L-moment (mean), t sample L-CV, t_3 sample L-skewness, t_4 sample L-kurtosis

for obtaining maximum benefits out of the regional frequency analysis (Lettenmaier et al. 1987; Stedinger and Lu 1995).

Considering the whole set of seven sites as a single region (Region S1), the heterogeneity measure "H" has been calculated. The computations involved in heterogeneity measure H are:

The group average L-moment ratios are

$$t^R = 0.1665,\ t_3^R = 0.0888,\ t_4^R = 0.1856, \tag{22}$$

the V measure calculated from the observed data is 0.0342 and the estimates of parameters of the regional Kappa distribution used for simulations are

$$\xi = 0.9758,\ \alpha = 0.1644,\ k = -0.0888,\ h = -1.0000. \tag{23}$$

For 500 simulated regions, μ_v and σ_v are 0.0147 and 0.0045 respectively. The value of H is 4.37 suggesting that the "Region S1" is definitely heterogeneous.

During the calculation of H for Region S1, an interesting feature of the data set has been observed. While fitting Kappa distribution to the regional weighted average L-moment ratios gives one of its parameter equal to -1, i.e. $h = -1$ (Eq. 23). In this case, Kappa distribution reduces to GLO distribution. The sites of the region have showed lower L-skewness with high L-kurtosis. For this reason, t_4^r is large relative to t_3^r. Also the data set have low outliers at each site except "Chashma" (Table 2). The problem might be due to the presence of these low outliers because, sometimes, the low outliers contribute to high L-kurtosis while reducing the L-skewness. Hosking and Wallis (1997) discussed such possibility and recommended to use GLO distribution for the simulations. The option has been evaded. The idea is to avoid at this stage, if possible, the use of a three-parameter distribution as parent distribution of the observed data set.

Secondly, in regional flood frequency studies, the interest is always in the estimation of quantiles in the extreme upper tail of the distribution and it could be beneficial to censor some of the smaller observations in the left tail (Wang 1990a, b, 1996; Zafirakou-Koulouris et al. 1998). Therefore, the low outliers have been discarded (eliminated) and the sample information has been re-summarized (recalculated) for seven sites of the "Region S1" and illustrated in Table 4. Zafirakou-Koulouris et al. (1998) used sample estimators of PPWMs and L-moments for the left censored (Type A') observations and worked on the artificial data sets with 20% and 80% level of censoring. The censoring level "c" used in the present study is too low

Table 4 Left censored sample L-moment and L-moment ratios of seven sites of the Indus River

Site Name	c	$n^{A'}$	$l_1^{A'}$	$t^{A'}$	$t_3^{A'}$	$t_4^{A'}$
Tarbela	0.0227	43	384767	0.0922	0.1046	0.0962
Kalabagh	0.0135	73	522373	0.1325	0.1661	0.2077
Chashma	0.0000	33	474263	0.1323	0.0471	0.1691
Taunsa	0.0217	45	466774	0.1299	0.0626	0.1244
Guddu	0.0097	102	658921	0.1695	0.1056	0.1938
Sukkur	0.0097	102	608692	0.1855	0.1069	0.1925
Kotri	0.0198	99	440121	0.1966	0.1395	0.1734

c fraction of censored observations, $n^{A'}$ remaining record length, $l_1^{A'}$ left censored first sample L-moment, $t^{A'}$, $t_3^{A'}$, and $t_4^{A'}$ type-A' left censored sample L-moment ratios

(almost negligible), therefore, assuming that the same relationships hold for different measures and parameters of different distributions as for the original (uncensored) data set.

After censoring the low outliers at the sites, the heterogeneity measure (H) has been recalculated and found to be 4.60 suggesting that the region is definitely heterogeneous. The estimates of parameters of the regional Kappa distribution used for simulations are now

$$\xi = 0.9598,\ \alpha = 0.1643,\ k = -0.0959,\ h = -0.8433. \tag{24}$$

Although, "Region S1" is still heterogeneous and needs subdivision to perform an accurate and reliable regional flood frequency analysis but the undue influence of the low outliers has been removed from the data set. As a result, a genuine four-parameter Kappa distribution has been used as parent distribution of the observed data to simulate regions for the calculation of H.

4.5.1 Subdivision of the Region S1

Generally, cluster analysis of the site characteristics is an appealing technique for the formation of regions. The flexibility of having subjective decisions at various stages makes it fairly popular among researchers. For the current problem, Ward's clustering method has been used with four site characteristics: AAP, APDM, site's latitude and site's longitude. Since there is no general guide for selecting the number of clusters (Fovel 1997); therefore, keeping in view the number of sites and geography of the region, it is sub-divided into two clusters. To avoid the influence of scale differences, all the variables (site characteristics) have been standardized. Manhattan Distance between two points has been used as a measure of similarity. The two clusters (regions) provided by the Ward's method are: "Region 1" consists of four sites (Tarbela, Kalabagh, Chashma and Taunsa) of the upper Indus basin and "Region 2" consists of three sites (Guddu, Sukkur and Kotri) of the lower Indus basin.

4.5.2 Heterogeneity Measure of the Sub-divided Regions

For Region 1 The value of H is found to be 1.17. The criteria of $H = 1$ for defining a homogenous region is somewhat arbitrary (Hosking and Wallis 1997). A little difference, above 1, can be tolerable. Success depends on the climatic and geographical structure of the study area. Region 1 showed a little heterogeneity, which is understandable because after the site "Tarbela" one major western tributary, the Kabul River, joins the Indus River. As a result, the site next to "Tarbela", i.e. "Kalabagh", showed high variations in its flows specially the L-skewness and L-kurtosis. Therefore, the geographical structure of the site "Kalabagh" contributes in the heterogeneity measure of Region 1 resulted in a value little above 1. Taking all this into account, the same combination (grouping) has been used in the further analysis. Many other studies have also performed regional frequency analysis with regions having value of H greater than 1, for example, Dinpashoh et al. (2004), Norbiato et al. (2007), Saf (2009), Jingyi and Hall (2004), Modarres (2007), Abida and Ellouze (2006) etc.

For Region 2 The group average L-moment ratios are

$$t^{R^{A'}} = 0.1837,\ t_3^{R^{A'}} = 0.1171,\ t_4^{R^{A'}} = 0.1867, \tag{25}$$

the V measure calculated from the observed data is 0.0111 and the estimates of the parameters of the regional Kappa distribution used for simulations are

$$\xi = 0.9648,\ \alpha = 0.1796,\ k = -0.1171,\ h = -1.0000. \tag{26}$$

For 500 simulated regions, μ_v and σ_v are 0.0110 and 0.0058 respectively. The value of H is 0.02 suggesting that "Region 2" is acceptably homogeneous.

Again for the calculation of "H" for Region 2, the fit of Kappa distribution to regional weighted average L-moment ratios reduces to GLO distribution. The sites in the region have longer record lengths and, geographically, lie in the lower basin of the Indus River. After the join of four major eastern tributaries, below "Taunsa", the flow of the Indus River becomes more complex by sharing the flow behavior of its eastern tributaries which may be a contributing factor for the sites of Region 2 having lower L-skewness and high L-kurtosis. Therefore, it may be possible that the data series of sites of Region 2 actually follows GLO distribution. Also, there is a problem of paucity of gauging sites and flow observations in this region. Further 10% or 20% censoring might also results in loss of available limited information. Therefore, following the recommendations of Hosking and Wallis (1997) to use GLO distribution for the simulations, the same region has been used in the further analysis.

4.6 Selection of a Regional Frequency Distribution

An L-moment ratio diagram for Region 1 and Region 2 is illustrated in Fig. 3. The plotted sample points are left censored type A' L-moment ratios. The regional

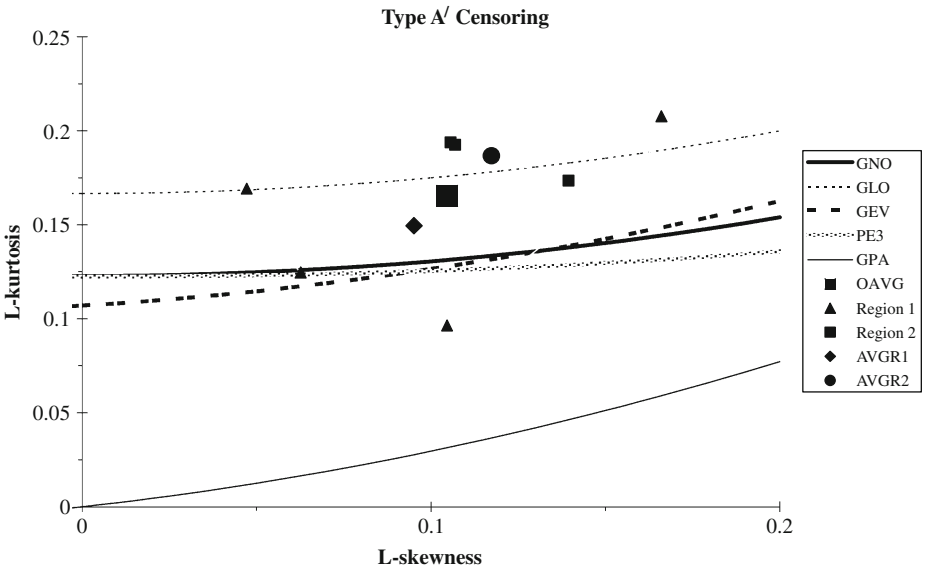

Fig. 3 L-moment ratio diagram for Region 1 and Region 2

average L-skewness and L-kurtosis for Region 1 (AVGR1) and Region 2 (AVGR2) are also plotted in Fig. 3. AVGR1 lies, approximately, in the middle of GNO and GLO distributions. Therefore, these two distributions can be considered as suitable candidates for Region 1. AVGR2 lies closest to the GLO distribution and far away from the other four distributions. Therefore, GLO is the only suitable distribution for Region 2. For interest, the overall average of L-skewness and L-kurtosis of the seven sites (OAVG) is also included in Fig. 3, which lies closest to the GLO distribution.

For the two regions, AWD measure values for various distributions are exemplified in Table 5. For Region 1, GLO distribution has the lowest AWD measure value. Therefore, it can be considered as the best-fitted distribution for Region 1. Furthermore, GNO distribution has AWD measure value close to the best-fitted distribution, therefore, can be considered as possible alternative. For Region 2, the best fitted distribution as per AWD statistic criteria is GLO. No other distribution has AWD measure value close to the best-fitted distribution.

For both regions, Table 5 also provides the $|Z^{DIST}|$-*measure* values for various three-parameter distributions. For Region 1, the four successful candidates for regional distribution are: GNO, GLO, GEV and PE3. Furthermore, the value of $|Z^{DIST}|$-*measure* is minimum for GLO distribution. For Region 2, only GLO has the value of $|Z^{DIST}|$-*measure* less than 1.64. For interest, the results for "Region S1" are also included in this section. Interestingly, GLO distribution has value of $|Z^{DIST}|$-*measure* exactly equal to "zero" and is the only distribution that has value of $|Z^{DIST}|$-*measure* less than 1.64.

The aforementioned results of the three measures suggest that Region 1 has four candidates: GNO, GLO, GEV and PE3 while Region 2 has one candidate: GLO as regional distribution. For both the regions, the results of $|Z^{DIST}|$ goodness-of-fit measure showed good agreement with AWD measure and L-moment ratio diagram.

After the selection of suitable regional frequency distribution(s), the parameters and quantiles of the respective distribution(s) have been calculated and the results are illustrated, for each region, in Table 6.

4.7 Assessment of the Accuracy of Regional Estimates

As more than one distribution has passed the goodness-of-fit criterion for Region 1, the most suitable will be the one that holds the robustness properties. Moreover, the aim of the study is not just to obtain a best-fitted distribution of the data series but to identify a distribution that provides more accurate quantile estimates especially in the extreme upper tail of the distribution. Therefore, a simulation study described in

Table 5 AWD and $|Z^{DIST}|$ values for different distributions

Region name	Number of sites	GNO	GLO	GEV	PE3	GPA
AWD measure values						
Region 1	4	0.0396	0.0351	0.0403	0.0433	0.1221
Region 2	3	0.0503	0.0175	0.0509	0.0587	0.1446
$\|Z^{DIST}\|$ measure values						
Region 1	4	0.99	0.66	1.10	1.21	4.67[a]
Region 2	3	2.64[a]	0.79	2.72[a]	2.92[a]	6.66[a]
Region S1	7	2.38[a]	0.00	2.51[a]	2.72[a]	7.60[a]

GPA is the generalized Pareto distribution
[a]Value of $|Z^{DIST}|$ that exceeds 1.64

Table 6 Estimates of parameters and quantiles of the candidate distribution(s) for each of the three regions

Distribution	Parameters				Quantile estimates with nonexceedance probability F					
	ξ	α	k	h	0.0100	0.1000	0.5000	0.9000	0.9900	0.9990
For Region 1										
GNO	0.976	0.213	−0.222	–	0.5890	0.7384	0.9760	1.2918	1.6247	1.9219
GLO	0.978	0.121	−0.108	–	0.5397	0.7413	0.9780	1.2781	1.6979	2.2198
GEV	0.906	0.193	0.098	–	0.5881	0.7383	0.9755	1.2958	1.6207	1.8746
PE3	1.000	0.221	0.661	–	0.5945	0.7370	0.9758	1.2942	1.6181	1.8937
For Region 2										
GLO	0.965	0.180	−0.117	–	0.3252	0.6162	0.9650	1.4160	2.0603	2.8783
For Region S1										
Kappa	0.960	0.164	−0.096	−0.843	0.4117	0.6674	0.9699	1.3629	1.9074	2.5671

– not applicable

Section 3.7, for assessing the accuracy of the estimated regional quantiles and growth curves has been conducted, for each of the sub-divided regions separately, and the results are discussed in the following section.

For Region 1 The first step in this procedure is to develop a region used as a basis for simulations that has resemblance with the realizations of the actual region, that is, in terms of the number of sites, record length at each site and regional average L-moment ratios. Also the simulated region has to include heterogeneity and intersite dependence, if exists. The L-moment ratios at the individual sites should be chosen to form a region whose heterogeneity is consistent with the heterogeneity measure calculated from the actual data. Region 1 has the value of H as 1.17 and four distributions: GNO, GLO, GEV and PE3, as possible candidates for regional distribution. The region also has a considerable amount of intersite dependence which was expected because all the sites belong to the same river (the Indus River). Correlations between sites have an average value of 0.82, therefore, the intersite dependence is incorporated in the simulations algorithm with correlation matrix having $\rho = 0.82$. To decide about the range of the L-CVs of the region used as a base for simulations, 100 simulations of the correlated GLO regions with record lengths the same as for the actual region show that when at-site L-CVs vary over a range of 0.0381, from 0.0939 at site 1 to 0.1320 at site 4 and L-skewness 0.1082, the average H value of the simulated regions is 1.13. This amount of heterogeneity of the simulated region resembles with the actual region. Therefore this region has been used as a base in the simulation procedure.

Ten thousand realizations of this region have been made and the regional L-moment algorithm has been used to fit each of the candidate distributions every time to the data generated at each realization. The whole procedure is repeated for GNO, GLO, GEV and PE3 distributions. From these simulations, the regional average relative bias, absolute relative bias and relative root mean square error for the estimated regional growth curves and quantiles are calculated and, for selected values of nonexceedance probability F, illustrated in Tables 7 and 8, respectively. Figure 4 shows the estimated regional growth curves together with their 90% error bounds.

Table 7 Accuracy measures for the estimated growth curves of Region 1, for the four candidate distributions

GNO						
F	0.010	0.100	0.500	0.900	0.990	0.999
$\hat{q}(F)$	0.589	0.738	0.976	1.292	1.625	1.922
Abs. Bias	0.069	0.036	0.003	0.024	0.041	0.052
Bias	0.009	0.006	0.000	−0.002	−0.001	0.002
RMSE	0.097	0.045	0.011	0.031	0.070	0.107
LB	0.531	0.706	0.959	1.255	1.487	1.650
UB	0.655	0.767	0.994	1.336	1.772	2.205
GLO						
F	0.010	0.100	0.500	0.900	0.990	0.999
$\hat{q}(F)$	0.540	0.741	0.978	1.278	1.698	2.220
Abs. Bias	0.083	0.035	0.002	0.023	0.044	0.060
Bias	0.008	0.006	0.000	−0.003	−0.002	0.006
RMSE	0.128	0.047	0.013	0.032	0.085	0.163
LB	0.472	0.707	0.959	1.237	1.508	1.733
UB	0.641	0.776	0.999	1.323	1.889	2.716
GEV						
F	0.010	0.100	0.500	0.900	0.990	0.999
$\hat{q}(F)$	0.588	0.738	0.976	1.296	1.620	1.875
Abs. Bias	0.069	0.036	0.003	0.024	0.041	0.050
Bias	0.010	0.005	0.000	−0.003	−0.001	0.006
RMSE	0.094	0.045	0.011	0.031	0.072	0.120
LB	0.534	0.706	0.958	1.260	1.473	1.559
UB	0.648	0.767	0.992	1.337	1.774	2.180
PE3						
F	0.010	0.100	0.500	0.900	0.990	0.999
$\hat{q}(F)$	0.595	0.737	0.976	1.294	1.618	1.894
Abs. Bias	0.068	0.036	0.003	0.024	0.041	0.051
Bias	0.010	0.006	0.000	−0.002	−0.002	−0.002
RMSE	0.098	0.045	0.011	0.032	0.065	0.092
LB	0.534	0.705	0.959	1.255	1.495	1.681
UB	0.664	0.765	0.994	1.337	1.753	2.136

$\hat{q}(F)$ is the estimated quantile function, "Abs. Bias", "Bias" and "RMSE" are regional average absolute relative bias, relative bias and relative root mean square error, respectively, for the estimated growth curves, LB and UB are the lower and upper 90 % error bounds, respectively, for the estimated growth curves

In Table 7, in terms of "Abs. Bias", the three distributions: GNO, GEV and PE3 have similar performances throughout. GLO distribution has a little higher value of "Abs. Bias" at F = 0.999 (1000 year return period). In terms of "Bias", there is nothing much to choose among the four distributions till F = 0.99 (100 year return period). At F = 0.999 (1000 year return period), GLO and GEV distributions have little higher values of "Bias" in comparison to GNO and PE3 distributions. Again in terms of "RMSE", the three distributions: GNO, GEV and PE3 have approximately similar performances till F = 0.99 (100 year return period). At F = 0.999 (1000 year return period), PE3 distribution has the lowest value of "RMSE" followed by the GNO and GEV distributions, respectively. However, GLO distribution has the highest values of "RMSE" at F = 0.99 (100 year return period) and F = 0.999 (1000 year return period). Figure 4 shows that in the upper tails of the distributions, GNO and PE3 have indistinguishable 90% error bounds while GEV distribution has a little wider 90% error bounds, especially the lower bound. Among the set of four candidates for regional distribution, GLO has the widest 90% error bounds, especially the upper bound. The accuracy measures for the estimated regional growth curves indicate that the performance of GLO distribution is not satisfactory while GNO and PE3

Table 8 Accuracy measures of the estimated quantiles of Region 1, for the four candidate distributions

GNO						
F	0.010	0.100	0.500	0.900	0.990	0.999
Abs. Bias	0.069	0.036	0.003	0.024	0.041	0.052
Bias	0.009	0.006	0.000	−0.002	−0.001	0.002
RMSE	0.101	0.053	0.032	0.045	0.078	0.113
GLO						
F	0.010	0.100	0.500	0.900	0.990	0.999
Abs. Bias	0.083	0.035	0.002	0.023	0.044	0.060
Bias	0.009	0.006	0.000	−0.003	−0.002	0.008
RMSE	0.135	0.056	0.030	0.047	0.098	0.175
GEV						
F	0.010	0.100	0.500	0.900	0.990	0.999
Abs. Bias	0.069	0.036	0.003	0.024	0.041	0.050
Bias	0.010	0.005	0.000	−0.002	−0.000	0.006
RMSE	0.097	0.053	0.032	0.045	0.079	0.125
PE3						
F	0.010	0.100	0.500	0.900	0.990	0.999
Abs. Bias	0.068	0.036	0.003	0.024	0.041	0.051
Bias	0.009	0.006	0.000	−0.002	−0.002	−0.002
RMSE	0.100	0.053	0.032	0.045	0.073	0.098

Various abbreviations are the same as explained in Table 7

distributions have comparable performances, therefore, either of them can be used for flood quantile estimates and the performance of GEV distribution is only a little inferior than GNO and PE3 distributions, especially in the extreme upper tail.

In Table 8, in terms of "Abs. Bias", only GLO distribution has a little higher value at F = 0.999 (1000 year return period). In terms of "Bias", there is nothing much to choose among the four distributions till F = 0.99 (100 year return period). At F = 0.999 (1000 year return period), GLO and GEV distributions have a little higher values than GNO and PE3 distributions. In terms of "RMSE", at F = 0.99

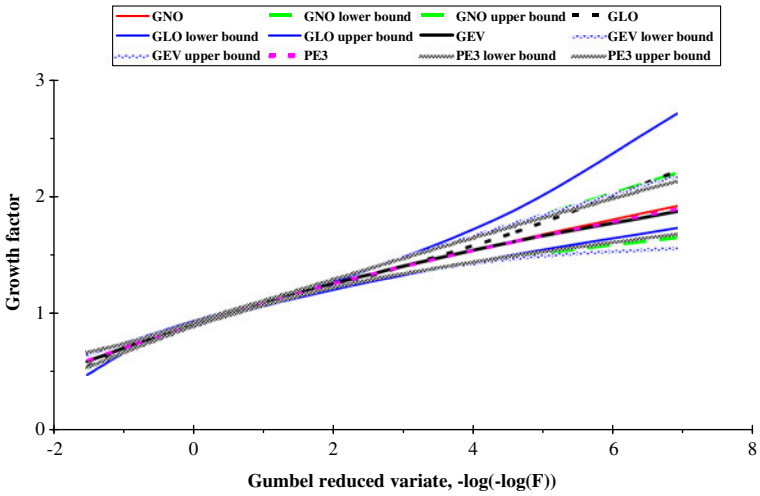

Fig. 4 Quantile functions of the four distributions fitted to the data of Region 1, with their 90% error bounds

Table 9 Accuracy measures for the estimated growth curve of Region 2

GLO						
F	0.010	0.100	0.500	0.900	0.990	0.999
$\hat{q}(F)$	0.325	0.616	0.965	1.416	2.060	2.878
Abs. Bias	0.090	0.026	0.002	0.013	0.022	0.030
Bias	−0.000	0.002	0.000	−0.001	0.000	0.009
RMSE	0.230	0.054	0.016	0.027	0.077	0.146
LB	0.247	0.575	0.941	1.364	1.823	2.272
UB	0.506	0.665	0.993	1.469	2.299	3.519

Various abbreviations are the same as explained in Table 7

(100 year return period) and F = 0.999 (1000 year return period), PE3 distribution has the lowest values followed by GNO, GEV and GLO distributions, respectively. The overall conclusion about the performance of the candidate distributions, based on the results of the accuracy measures of the estimated regional quantiles, is same to that resulted from the accuracy measures for the estimated regional growth curves.

For Region 2 Similar procedure has been repeated for Region 2 which has the value of H as 0.02 and GLO as candidate for regional distribution. Correlations between sites have an average value of 0.83, therefore, the interiste dependence is incorporated in the simulations algorithm with correlation matrix having $\rho = 0.83$. For the range of L-CVs of the region used as a base region for simulations, 100 simulations of the correlated GLO regions with record lengths the same as for the actual region show that when at-site L-CVs vary over a range of 0.0230, from 0.1723 at site 1 to 0.1953 at site 3 and L-skewness 0.1171, the average H value of the simulated regions is 0.06. This region has been used as a base in the simulation procedure. Ten thousand realizations of this region have been made with GLO as parent distribution and from these simulations accuracy measures have been calculated for the estimated regional growth curve and quantiles and are exemplified in Tables 9 and 10, respectively. Figure 5 shows the estimated regional growth curve together with its 90% error bounds.

Fortran routines of Hosking (2000) have been used to calculate different measures related to regional frequency analysis (discordancy, heterogeneity and Z^{DIST}) and measures of accuracy for the estimated regional growth curves and quantiles.

4.8 Standard Errors of the Estimated At-site Quantiles

The simulations procedure (algorithm) of Hosking and Wallis (1997), for the assessment of accuracy, principally, provides the "Abs. Bias", "Bias" and "RMSE" for

Table 10 Accuracy measures of the estimated quantiles of Region 2

GLO						
F	0.010	0.100	0.500	0.900	0.990	0.999
Abs. Bias	0.090	0.026	0.002	0.013	0.022	0.030
Bias	0.002	0.002	0.000	−0.001	0.001	0.010
RMSE	0.241	0.065	0.033	0.045	0.092	0.161

Various abbreviations are the same as explained in Table 7

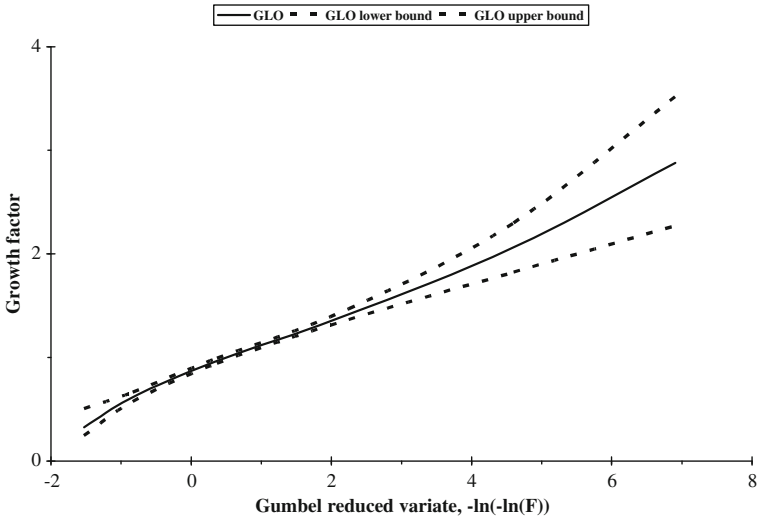

Fig. 5 Quantile function of the GLO distribution fitted to the data of Region 2, with its 90% error bounds

the regional estimates. However, the results can be utilized further, to obtain the standard errors of the estimated quantiles at each site of the region. The relationship provided in Hosking and Wallis (1997; Section 7.2) has been explored for this purpose. According to them;

$$\text{var}\left\{\hat{Q}_i(F)\right\} \approx \{x(F;\theta_0)\}^2 \,\text{var}\left(\hat{\mu}_i\right) + \mu_i^2 \text{var}\left\{x\left(F;\hat{\theta}\right)\right\}. \tag{27}$$

For the above relationship, the two terms on the right hand side of the equality; $x(F;\theta_0)$ and μ_i, have been replaced by their estimators (respectively, the estimated regional growth curve for nonexceedance probability F and sample mean at site i). The term $\text{var}\left(\hat{\mu}_i\right)$ has been obtained analytically, i.e. $\text{var}\left(\hat{\mu}_i\right) = \hat{\sigma}_i^2/n$ (where $\hat{\sigma}_i^2$ is the sample variance at site i). The fourth term $\text{var}\left\{x\left(F;\hat{\theta}\right)\right\}$, for the respective values of nonexceedance probability F, has been obtained from the results of the simulations procedure for the assessment of accuracy of the regional estimates, i.e. $\text{var}\left\{x\left(F;\hat{\theta}\right)\right\} = RMSE\left\{x\left(F;\hat{\theta}\right)\right\} - \left[Bias\left\{x\left(F;\hat{\theta}\right)\right\}\right]^2$. Taking square root of the quantity (the term on the left hand side of Eq. 27), obtained after putting the values of the terms on the right hand side, provides standard errors of the estimated at-site quantiles through regional approach.

For various values of nonexceedance probability F, quantile estimates at each site of the sub-divided regions have been obtained using Eq. 14. For each region, the representative robust regional distribution, i.e. PE3 distribution for Region 1 and GLO distribution for Region 2, has been used and the results are exemplified in the Table 11.

Table 11 At-site quantile estimates alongwith their standard errors

F	0.100	0.500	0.900	0.990	0.999
Tarbela					
$\hat{Q}_i(F)$	283573	375533	497888	622553	728749
S.E. $\left(\hat{Q}_i(F)\right)$	18537	10205	17394	29357	39714
Kalabagh					
$\hat{Q}_i(F)$	384989	509836	675951	845200	989374
S.E. $\left(\hat{Q}_i(F)\right)$	25766	15668	25531	41662	55755
Chashma					
$\hat{Q}_i(F)$	349532	462881	613696	767358	898254
S.E. $\left(\hat{Q}_i(F)\right)$	25535	19651	29333	43999	57049
Taunsa					
$\hat{Q}_i(F)$	344012	455571	604006	755240	884070
S.E. $\left(\hat{Q}_i(F)\right)$	23947	16495	25577	39937	52617
Guddu					
$\hat{Q}_i(F)$	405895	635859	933032	1357377	1896375
S.E. $\left(\hat{Q}_i(F)\right)$	37640	22031	33493	65418	112019
Sukkur					
$\hat{Q}_i(F)$	374954	587388	861908	1253906	1751816
S.E. $\left(\hat{Q}_i(F)\right)$	35139	21848	33065	62767	106159
Kotri					
$\hat{Q}_i(F)$	271115	424717	623211	906649	1266668
S.E. $\left(\hat{Q}_i(F)\right)$	25670	16805	25343	47004	78639

$\hat{Q}_i(F)$ are the at-site quantile estimates and S.E. $\left(\hat{Q}_i(F)\right)$ are the standard errors of the estimated at-site quantiles

5 Comparison of the Estimated Quantiles Using At-site and Regional Approach

The extension, of the results of simulation experiments for obtaining the standard errors of the estimated flood quantiles at each site of the sub-divided homogeneous regions, has actually facilitated to compare the results of the regional study with that of the at-site analysis. For example, Memon (2007) compared the fit of PE3 and Log-Pearson III (LPE3) distributions using annual peak flood data of site "Kotri", of the Indus River. Three parameter estimation methods: MOM, MLM and PWM, were used and he concluded that both PE3 and LPE3 distributions with MLM provided minimum standard errors of the estimated quantiles, for various return periods till 100 years. For F = 0.9 (10 year return period) and F = 0.99 (100 year return period), the standard errors of the estimated quantiles at site Kotri, of the present study and the previous study of Memon (2007), have been compared in Fig. 6. Figure 6 shows that standard errors of the estimated quantiles, resulted from the regional flood frequency analysis are clearly minimum. Considerable difference has been observed at F = 0.9 (10 year return period) and the gap becomes even wider in the upper tail of the distribution.

Another at-site frequency analysis conducted by Muhammad and Afreen (2007) using Gumbel and GEV distributions showed that GEV distribution with parameters estimated by PWM proved to be the best-fitted for the AMP flows of sites Kalabagh and Kotri. The present study used five three-parameter distributions, including GEV,

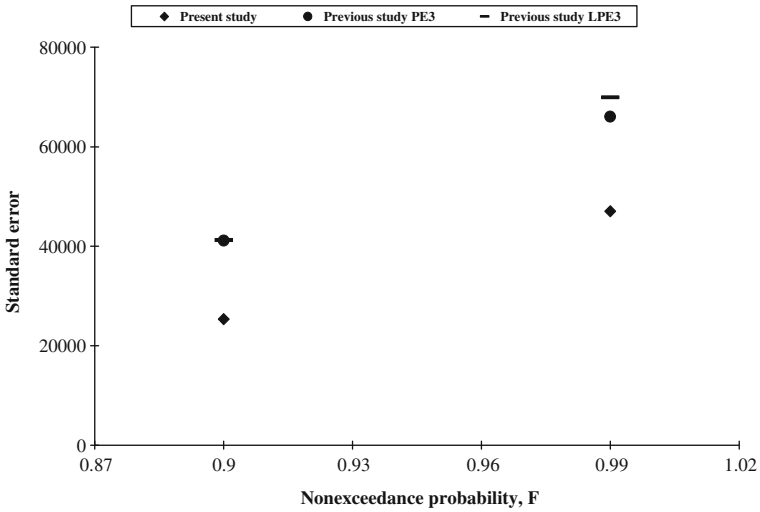

Fig. 6 Comparison of standard errors of the estimated quantiles at site "Kotri"

in the analysis. The results showed that the performance of PE3 distribution for the site Kalabagh and GLO distribution for the site Kotri, is relatively better than GEV distribution.

6 Summary and Conclusions

For a country, with an agro based economy and having threats of water scarcity, the need of accurate and reliable estimates of flood quantiles is immense. Moreover, the Indus River provides the key water resources for the economy of Pakistan, especially the "Breadbasket" of the Punjab province, which accounts for most of the nation's agricultural production, and the Sindh. Therefore, this study is conducted to find out reliable flood quantile estimates, using commonly adopted procedure in various studies across the world, for the design capacity of the proposed hydraulic structures (for example, Kalabagh) and to reassess the risks associated to the hydraulic structures already in place (for example, Tarbela etc) on the Indus River. Previously documented studies in Pakistan concentrated on the at-site flood frequency analysis. The current effort, to the best of author's knowledge, is the first application of L-moments based regional flood frequency analysis of the seven gauged stations located on the Indus River main stream. Data series of the seven sites satisfy various assumptions of the adopted procedure for the analysis. Few sites have low outlier(s) because of the arid or semi-arid nature of the study area but their undue influence has been removed using the idea of left censored type A' PPWMs. The region, consisting of seven sites, is heterogeneous which may be attributed to the diversified topography (as shown by the site characteristics, Table 1) of the study area. The Indus River flows through the entire country (from North to South direction, Fig. 1), with a length of approximately 2,066 km. Moreover, all the other rivers of the system join it at some stage. Thus, by covering a large area with diversified geographical and

climatic conditions and by sharing the flow behavior of other rivers, the Indus River becomes a complex and mighty river. In this situation, identification of homogeneous regions becomes difficult; still, couple of homogeneous region has been identified using Ward's clustering method based on the site characteristics only. The results of L-moment ratio diagram, AWD and Z^{DIST} measures show that Region 1 has four candidates; GNO, GLO, GEV and PE3, while, Region 2 has only one candidate; GLO as regional distribution. For both regions, accuracy of the estimated regional growth curves and quantiles have been assessed using Monte Carlo simulations.

The results of the simulation experiments show that for Region 1, among the four candidates, two distributions: GNO and PE3 have comparable performances. Not only these distributions have indistinguishable growth curves but also have similar 90% error bounds. Therefore, either of the distributions can be used for flood quantile estimates at each site of Region 1, for instance, PE3 distribution has been used. For Region 2, GLO distribution can be used for the estimation of flood quantiles at each site. This also shows that the choice of using GLO as parent distribution, for the calculation of heterogeneity measure (H) for Region 2, seems appropriate.

The simulations study, related to the accuracy measures of the estimated regional growth curves and quantiles has shown that, for both regions, values of the "RMSE" of the estimated quantiles are greater than or nearly equal to the values of the "RMSE" of the estimated growth curves, corresponding to the same return periods. This occurs, because the "RMSE" of the estimated quantiles includes the variability of the estimated index flood (mean at each site). Similar results have been reported by Saf (2009).

After the selection of the most appropriate robust distribution for each region, one can compare the slopes of their growth curves. The regional growth curves for the sub-divided regions of the Indus River are presented in Fig. 7. The estimates of quantiles for F = 0.5, for all the regions, are less than unity. Guttman et al. (1993) has

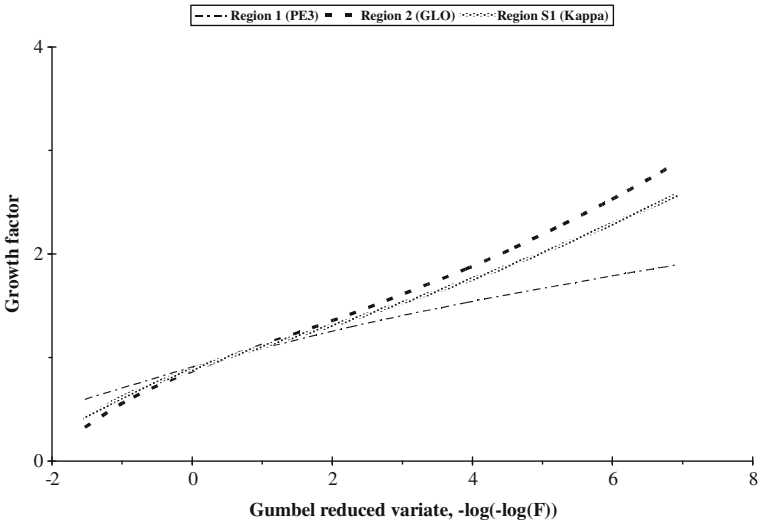

Fig. 7 Growth curves of sub-divided regions of the Indus River

reported similar results for the arid regions in USA. Dinpashoh et al. (2004) has also experienced similar behavior of quantiles for the seven precipitation climates of Iran. For interest, the growth curve of Kappa distribution for "Region S1" is also included in Fig. 7. The slopes of the growth curves of Region 2 and Region S1 are closer to each other. Sites of Region 2 have shown higher variations in their AMP flows, in terms of L-CV. Flow behavior of the eastern tributaries is a contributing factor in the variations of AMP flows of the sites of Region 2.

The results, of the simulations study for the accuracy measures of the regional estimates, have been extended to obtain the standard errors of the estimated flood quantiles at each site of the sub-divided homogeneous regions. This extension has facilitated the comparison of the quality of estimates of the regional study with the at-site analysis. This procedure can be adopted; in general, to compare the quality of quantile estimates obtained at each site from L-moments based regional analysis to that of other procedures of frequency analysis of extreme events.

Acknowledgements The author would like to acknowledge the support and facilitation provided by Water and Power Development Authority (WAPDA), Lahore and National Engineering Services Pakistan (Pvt.) Limited (NESPAK), Lahore for the retrieval of the hydrological data for the study. My special thanks to Dr. J.R.M. Hosking, T. J. Watson research centre, New York, for his useful suggestions during the research work. My gratitude also to the anonymous reviewers, whose constructive comments and suggestions improved the quality of the paper.

References

Abida H, Ellouze M (2006) Hydrological delineation of homogeneous regions in Tunisia. Water Resour Manag 20:961–977

Alila Y (1999) A hierarchical approach for the regionalization of precipitation annual maxima in Canada. J Geophys Res 104(31):31645–31655

Alila Y (2000) Regional rainfall depth-duration-frequency equations for Canada. Water Resour Res 36:1767–1778

Ben-Zvi A, Azmon B (1997) Joint use of L-moment diagram and goodness of fit test: a case study of diverse series. J Hydrol 198(1–4):245–259

Bradley JV (1968) Distribution-free statistical tests. Prentice-Hall, Englewood cliffs

Burn DH (1990) Evaluation of regional flood frequency analysis with a region of influence approach. Water Resour Res 26:2257–2265

Castellarin A, Burn DH, Brath A (2008) Homogeneity testing: how homogeneous do heterogeneous cross-correlated regions seem? J Hydrol 360:67–76

Chernoff H, Gastwirth JL, Johns MV (1967) Asymptotic distribution of linear combinations of functions of order statistics with applications to estimation. Ann Math Stat 38(1):52–72

Cunnane C (1988) Methods and merits of regional flood frequency analysis. J Hydrol 100:269–290

David HA (1968) Gini's mean difference rediscovered. Biometrika 55:573–575

Dinpashoh Y, Fakheri-Fard A, Moghaddam M, Jahanbakhsh S, Mirnia M (2004) Selection of variables for the purpose of regionalization of Iran's precipitation climate using multivariate methods. J Hydrol 297:109–123

Durrans SR (1996) Low-flow analysis with a conditional Weibull tail model. Water Resour Res 32(6):1749–1760

Durrans SR, Tomic S (1996) Regionalization of low-flow frequency estimates: an Alabama case study. Water Resour Bull 32:23–37

Elamir EA, Seheult AH (2001) Control charts based on linear combinations of order statistics. J Appl Statist 28:457–468

Eslamian SS, Feizi H (2007) Maximum monthly rainfall analysis using L-moments for an Arid Region in Isfahan Province, Iran. J Appl Meteorol Climatol 46(4):494–503

Fovel RG (1997) Consensus clustering of U.S. temperature and precipitation data. J Climatol 10:1405–1430

Government of Pakistan (2001) National flood protection plan-III (A draft prepared by Federal Flood Commission). Ministry of Water and Power, Islamabad
Greenwood JA, Landwehr JM, Matalas NC, Wallis JR (1979) Probability weighted moments: definition and relation to parameters of several distributions expressible in inverse form. Water Resour Res 15:1049–1054
Groupe de recherché en hydrologie statistique (GREHYS) (1996a) Presentation and review of some methods for regional flood frequency analysis. J Hydrol 186:63–84
Groupe de recherché en hydrologie statistique (GREHYS) (1996b) Inter-comparison of regional flood frequency procedures for Canadian rivers. J Hydrol 186:85–103
Grubbs F, Beck G (1972) Extension of sample sizes and percentage points for significance tests of outlying observations. Technometrics 14(4):847–854
Guttman NB, Hosking JRM, Wallis JR (1993) Regional precipitation of quantile values for the continental United States computed from L-moments. J Climate 6:2326–2340
Hosking JRM (1990) L-moments: analysis and estimation of distributions using linear combinations of order statistics. J R Stat Soc, B 52:105–124
Hosking JRM (1995) The use of L-moments in the analysis of censored data. In: Balakrishnan N (ed) Recent advances in life-testing and reliability, Chap. 29. CRC, Boca Raton, pp 546–560
Hosking JRM (2000) Fortran routines for use with the methods of L-moments. Version 3.03. IBM Research Division. T.J. Watson Research Centre, Yorktown Heights
Hosking JRM, Wallis JR (1993) Some statistics useful in regional frequency analysis. Water Resour Res 29:271–281. Correction: 1995. Water Resour Res 31:251
Hosking JRM, Wallis JR (1997) Regional frequency analysis: an approach based on L-moments. Cambridge University Press, New York
Hussain N (2000) Regional flood analysis for the Indus River catchment. M.Sc. thesis, National Library of Engineering Sciences, UET, Lahore, Pakistan, Call No. 627.4N23R
Hussain Z, Pasha GR (2009) Regional flood frequency analysis of the seven sites of Punjab, Pakistan, using L-moments. Water Resour Manag 23:1917–1933
Jehanzeb (2004) Evaluation of flooding hazards of Soan River in Rawalpindi area. M.Sc. thesis, National Library of Engineering Sciences, UET, Lahore, Pakistan, Call No. 627.4J55E
Jingyi Z, Hall MJ (2004) Regional flood frequency analysis for the Gan-Ming River basin in China. J Hydrol 296:98–117
Kendal MG, Stuart A (1968) The advanced theory of statistics, vol. 3: design and analysis, and time Series
Khattak HA (1994) Probability analysis of peak runoff and rainfall for selected catchments of NWFP. M. Sthesis, National Library of Engineering Sciences, UET, Lahore, Pakistan, Call No. 551.4880954912K94P
Kroll CK, Vogel RM (2002) Probability distribution of low streamflow series in the United States. J Hydrol Eng 7(2):137–146
Lettenmaier DP, Wallis JR, Wood EF (1987) Effect of regional heterogeneity on flood frequency estimation. Water Resour Res 23(2):313–323
Memon AG (2006) Statistical study of flood frequency analysis of Indus River at various barrages in Sindh. Ph.D. thesis, Shah Abdul Latif University, Khairpur, Pakistan
Memon AG (2007) Fitting Pearson III and Log-Pearson III distributions on floods data of Indus River at Kotri. Pak J Stat 23(2):157–169
Modarres R (2007) Regional frequency distribution type of low flow in north of Iran by L-moments. Water Resour Manag 22:823–841. doi:10.1007/s11269-007-9194-8
Muhammad F, Afreen S (2007) Modeling annual maximum peak flows at various dams and barrages in Pakistan. J Hydrol Hydromech 55(1):43–53
Musa M (1999) An appraisal of method of moments as applicable to water resource processes. M.Sc. thesis, National Library of Engineering Sciences, UET, Lahore, Pakistan, Call No. 627M98A
Nguyen V-T-V, Pandey G (1996) A new approach to regional estimation of floods in Quebec. In: Delisle CE, Bouchard MA (eds) Proceedings of the 49th Annual Conference of the CWRA, Quebec City, 26-28 June. Collection Environnement de 1'U. de M., pp 587–596
Norbiato D, Borga M, Sangati M, Zanon F (2007) Regional frequency analysis of extreme precipitation in the eastern Italian Alps and the August 29, 2003 flash flood. J Hydrol 345:149–166
Ouarda TBMJ, Girard C, Cavadias GS, Bobee B (2001) Regional flood frequency estimation with canonical correlation analysis. J Hydrol 254:157–173
Pakistan Meteorological Department (2010) Climate information, link: http://www.pakmet.com.pk/cdpc/Pakistan_mean_rainfall.pdf
Pakistan Water Gateway (2008) Indus basin, link: http://www.waterinfo.net.pk/pdf/indusbasin.PDF

Pandey MD, Gelder PHAJMV, Vrijling JK (2001) The estimation of extreme quantiles of wind velocity using L-moments in the peaks-over-threshold approach. Struct Saf 23(2):179–192
Peel MC, Wang QJ, Vogel R, McMahon TA (2001) The utility of L-moment ratio diagrams for selecting a regional probability distribution. Hydrol Sci J 46(1):147–155
Rao AR, Hamed KH (2000) Flood frequency analysis. CRC, London
Saf B (2009) Regional flood frequency analysis using L-moments for the West Mediterranean region of Turkey. Water Resour Manag 23:531–551
Shujah T (2009) Impact of glacier melting on flood generation in Indus River. M.Sc. thesis, National Library of Engineering Sciences, UET, Lahore, Pakistan, Call No. 536.42T13I
Sillitto G (1969) Derivation of approximants to the inverse distribution function of a continuous univariate population from the order statistics of a sample. Biometrika 56(3):641–650
Smithers JC, Schulze RE (2001) A methodology for the estimation of short duration desigh storms in South Africa using a regional approach based on L-moments. J Hydrol 241(1–2):42–52
Stedinger JR, Lu LH (1995) Appraisal of regional and index flood quantile estimators. Stoch Hydrol Hydraul 9(1):49–75
Stedinger JR, Tasker G (1986) Regional hydrologic analysis, 2, model-error estimators, estimation of sigma and log Pearson type 3 distributions. Water Resour Res 22:1487–1499
Vogel RM, Fennessey NM (1993) L-moments should replace product moments diagrams. Water Resour Res 29(6):1745–1752
Wang QJ (1990a) Estimation of the GEV distribution from censored samples by method of partial probability weighted moments. J Hydrol 120:103–114
Wang QJ (1990b) Unbiased estimation of probability weighted moments and partial probability weighted moments from systematic and historical flood information and their application to estimating the GEV distribution. J Hydrol 120:115–124
Wang QJ (1996) Using partial probability weighted moments to fit the extreme value distributions to censored samples. Water Resour Res 32(6):1767–1771
Yang T, Xu C, Shao Q, Chen X (2009) Regional flood frequency and spatial patterns analysis in the Pearl River Delta region using L-moments approach. Stoch Environ Res Risk Assess 24:165–182. doi:10.1007/s00477-009-0308-0
Zafirakou-Koulouris A, Vogel RM, Craig SM, Habermeier J (1998) L-moment diagrams for censored observations. Water Resour Res 34(5):1241–1249